Published in final edited form as:
J Membr Biol. 2009 March ; 228(1): 15–31. doi:10.1007/s00232-009-9155-7.

Concentration-Dependent Effects on Intracellular and Surface pH of Exposing *Xenopus* oocytes to Solutions Containing NH_3/NH_4^+

Raif Musa-Aziz,
Department of Cellular and Molecular Physiology, Yale University School of Medicine, New Haven, CT 06520, USA

Department of Physiology & Biophysics, Case Western Reserve University, 10900 Euclid Avenue, Cleveland, OH 44106, USA, raif.aziz@case.edu

Lihong Jiang,
Department of Diagnostic Radiology and Magnetic Resonance Research Center, Yale University School of Medicine, New Haven, CT 06520, USA

Li-Ming Chen,
Department of Cellular and Molecular Physiology, Yale University School of Medicine, New Haven, CT 06520, USA

Kevin L. Behar, and
Department of Psychiatry and Magnetic Resonance Research Center, Yale University School of Medicine, New Haven, CT 06520, USA

Walter F. Boron
Department of Cellular and Molecular Physiology, Yale University School of Medicine, New Haven, CT 06520, USA

Department of Physiology & Biophysics, Case Western Reserve University, 10900 Euclid Avenue, Cleveland, OH 44106, USA, walter.boron@case.edu

Abstract

Others have shown that exposing oocytes to high levels of NH_3/NH_4^+ (10–20 mM) causes a paradoxical fall in intracellular pH (pH_i), whereas low levels (e.g., 0.5 mM) cause little pH_i change. Here we monitored pH_i and extra-cellular surface pH (pH_S) while exposing oocytes to 5 or 0.5 mM NH_3/NH_4^+. We confirm that 5 mM NH_3/NH_4^+ causes a paradoxical pH_i fall ($-\Delta pH_i \cong 0.2$), but also observe an abrupt pH_S fall ($-\Delta pH_S \cong 0.2$)—indicative of NH_3 influx—followed by a slow decay. Reducing [NH_3/NH_4^+] to 0.5 mM minimizes pH_i changes but maintains pH_S changes at a reduced magnitude. Expressing AmtB (bacterial Rh homologue) exaggerates $-\Delta pH_S$ at both NH_3/NH_4^+ levels. During removal of 0.5 or 5 mM NH_3/NH_4^+, failure of pH_S to markedly overshoot bulk extracellular pH implies little NH_3 efflux and, thus, little free cytosolic NH_3/NH_4^+. A new analysis of the effects of NH_3 vs. NH_4^+ fluxes on pH_S and pH_i indicates that (a) NH_3 rather than NH_4^+ fluxes dominate pH_i and pH_S changes and (b) oocytes dispose of most incoming NH_3. NMR studies of oocytes exposed to ^{15}N-labeled NH_3/NH_4^+ show no significant formation of glutamine but substantial NH_3/NH_4^+ accumulation in what is likely an acid intracellular compartment. In conclusion, parallel measurements of pH_i and pH_S demonstrate that NH_3 flows across the plasma membrane and provide new insights into how a protein molecule in the plasma membrane—AmtB—enhances the flux of a gas across a biological membrane.

Correspondence to: Raif Musa-Aziz; Walter F. Boron.

Keywords

NH_3 permeability; Surface pH measurement; *Xenopus* oocytes; AmtB

The movement of NH_3 across cell membranes is important for several physiological processes, including nitrogen metabolism by the liver and acid-base transport by the kidney. In 1897, Overton—monitoring the precipitation of tannins in the algae *Spirogyra*—demonstrated that it is NH_3 rather than NH_4^+ that readily crosses the cell membrane. Later, Warburg (1922), Harvey (1911), and Jacobs (1922) reached similar conclusions working on a variety of preparations and using different approaches to show that the influx of NH_3 produces a rise in internal pH (pH_i). More recently, work with pH-sensitive microelectrodes by Boron and De Weer (1976b) on squid giant axons demonstrated that, although the influx of the weak base NH_3 causes a large and rapid increase in pH_i, the lower influx of the weak acid NH_4^+ produces a slow fall in pH_i during the "plateau phase" of the NH_3/NH_4^+ exposure. Moreover, this influx of NH_4^+ during the exposure to extracellular NH_3/NH_4^+ leads to large undershoot of the original pH_i, once the NH_3/NH_4^+ is removed from the extracellular solution. This effect is the basis of the widely used "ammonium prepulse" technique that they introduced (Boron and De Weer 1976a, 1976b).

Aickin and Thomas (1977) subsequently showed that the uptake of NH_4^+ can be so powerful in mammalian skeletal muscle that the alkalinizing effect of NH_3 entry is barely detectable. Kikeri et al. (1989) made similar observations when introducing NH_3/NH_4^+ into the lumen of the renal thick ascending limb. Waisbren et al. (1994) were the first to definitively identify a gas-impermeable membrane, showing that neither NH_3 nor NH_4^+ (nor CO_2 nor HCO_3^-) could cross the apical membranes of gastric gland cells.

In small-diameter *Xenopus* oocytes (Keicher and Meech 1994), an exposure to 20 mM extracellular NH_3/NH_4^+ produces the classic biphasic rise in pH_i, followed by a fall. However, in large-diameter oocytes (Burckhardt and Frömter 1992; Keicher and Meech 1994), an exposure to 20 mM NH_3/NH_4^+ causes a paradoxical fall in pH_i and a strong positive shift in membrane potential (V_m). To explain the above effect, Burckhardt and Frömter hypothesized that NH_4^+ enters via a nonselective cation channel, dissociates to form $NH_3 + H^+$, possibly followed by sequestration of NH_3 in lipid stores. This model calls for negligible NH_3 permeability and accounts for the then-available data. Keicher and Meech found that the NH_3/NH_4^+-induced fall in pH_i requires extracellular Cl^- and proposed that the fall in pH_i is due in part to an Na/K/Cl cotransporter that carries NH_4^+ in place of K^+. However, the acidification was only slightly inhibited by Na^+ removal or by bumetanide. Moreover, Na/NH_4/Cl cotransport would not account for the positive shift in V_m, which was not abolished by Cl^- removal. Note that, in the Keicher-Meech model, the pH_i decrease would require that the NH_4^+ influx be accompanied by an NH_3 efflux, as outlined originally by Boron and De Weer, and lead to a buildup of cytosolic NH_4^+. However, if the oocytes could mediate NH_3 efflux, then NH_3/NH_4^+ removal would lead to a rapid decrease in pH_i, which is not observed. Thus, although the Keicher-Meech model has interesting features, it cannot account for all of the then-available observations.

Later, Bakouh et al. (2006) confirmed that *Xenopus* oocytes exposed to relatively high levels of NH_3/NH_4^+ (i.e., 10 mM) exhibit the fall in pH_i noted above, but also found that oocytes exposed to only 0.5 mM NH_3/NH_4^+ exhibited no change in pH_i and no substantial induced inward current (related to net entry of positive charge, namely, NH_4^+) (Bakouh et al. 2004, 2006). The above results are consistent with the hypothesis that the NH_3/NH_4^+-induced fall in pH_i and positive shift in V_m are due to a low-affinity NH_4^+- uptake mechanism that is, to some extent, Cl^- dependent and that is largely inoperative at 0.5 mM NH_3/NH_4^+.

More recently, it has become clear that the AmtB/Rh family of membrane proteins can serve as a conduit for NH_3/NH_4^+. The crystal structures of several prokaryotic family members are consistent with the idea that NH_3 passes through pores in each of the three monomers of the homotrimer (Fabiny et al. 1991; Soupene et al. 2002; Khademi et al. 2004; Zheng et al. 2004; Andrade et al. 2005; Khademi and Stroud 2006; Conroy et al. 2007). In *Xenopus* oocytes expressing RhCG, Bakouh et al. (2004, 2006) found that an exposure to 0.5 mM NH_3/NH_4^+ produced a rapid, small, and short-lived alkalinization that was followed by a slow, small, and sustained acidification. These authors proposed that the transient pH_i increase reflects the influx of NH_3, whereas the subsequent pH_i decrease reflects NH_4^+ influx in concert with NH_3 efflux— all fluxes mediated by RhCG. However, as noted in connection with the Keicher-Meech data, if RhCG could mediate NH_3 efflux—and if appreciable NH_4^+ accumulated inside the oocyte during the preceding NH_3/NH_4^+ exposure—then NH_3/NH_4^+ removal should have led to a large and rapid pH_i decrease, which was not observed.

The purpose of the present work was to elucidate the movements of NH_3 vs. NH_4^+ across the plasma membrane—and the potential role of Amt in mediating these fluxes—using the oocyte as a model system. An ancillary goal, necessary to verify our interpretation of the data, was to explore the unusual handling of NH_3/NH_4^+ by the oocyte. Our approach was to extend to NH_3 fluxes a technique that we introduced earlier to assess CO_2 fluxes across the oocyte membrane (Endeward et al. 2006; Musa-Aziz et al. 2009). In the earlier work, we pushed a blunt pH microelectrode against the oocyte membrane and found that an exposure to CO_2/HCO_3^- causes a transient rise in surface pH (pH_S). First observed in 1984 by De Hemptinne and Huguenin (1984), who worked on rat soleus muscle, this rise in pH occurs as CO_2 uptake causes the depletion of CO_2 at the cell surface, leading to the reaction $HCO_3^- + H^+ \rightarrow CO_2 + H_2O$. In 1986, Chesler (1986) found that exposing lamprey neurons to the weak base NH_3 causes a transient decrease in extracellular pH. We hypothesized that a hitherto unseen flux of NH_3 into the oocyte would deplete NH_3 at the extracellular surface. This depletion would lead to the reaction $NH_4^+ \rightarrow NH_3 + H^+$, which would lower pH_S and also partially replenish surface NH_3 (Fig. 1). We found that exposures to both 5 and 0.5 mM elicited transient pH_S decreases, and that these decreases were augmented by the expression of AmtB. The exposure to 5 mM NH_3/NH_4^+ also caused a paradoxical fall in pH_i; thus, in this case, the pH fell on both sides of the membrane. We have developed a model that allows us to predict the direction in which fluxes of NH_3 and NH_4^+ would affect pH on both sides of the membrane. Guided by this model and our new pH_S data, we conclude that (a) earlier models of how 20 mM NH_3/NH_4^+ affects oocyte pH_i are incomplete; (b) in oocytes exposed to 5 or 0.5 mM NH_3/NH_4^+, the influx of NH_3 produces the dominant effects on pH_S (though we cannot rule out substantial NH_4^+ fluxes); (c) oocytes metabolize or sequester incoming NH_3; and (d) AmtB enhances permeability to NH_3 more than that to NH_4^+.

Methods

Expression in *Xenopus* Oocytes

cRNA Synthesis—As described elsewhere (Musa-Aziz et al. 2009), we used AmtB that we had tagged at the C terminus with EGFP (enhanced green fluorescent protein). We then used *Not*I to linearize AmtB cDNA constructs in pGH19, purified linearized cDNA using the QIAquick PCR purification kit (Qiagen Inc., Valencia, CA), transcribed capped cRNA using the T7 mMessage mMachine kit (Ambion, Austin, TX), and, finally, purified and concentrated cRNA using the RNeasy MinElute RNA Cleanup Kit (QIAGEN). We determined the RNA concentration using ultraviolet absorbance and assessed quality using gel electrophoresis.

Xenopus Oocyte Isolation—We surgically removed ovaries from anesthetized frogs, separated the oocytes using a collagenase treatment (Romero et al. 1998; Toye et al. 2006),

selected Stage V–VI oocytes, and stored them until use at 18°C in OR3 medium supplemented with 500 U of penicillin and 500 U of streptomycin.

Microinjection of cRNAs—One day after isolation, we injected oocytes with either 25 ng of cRNA encoding AmtB-EGFP cRNA (50 nl of a 0.5 ng/nl cRNA solution) or 50 nl of sterile water (Ambion, Austin, TX) in the case of control ("H_2O") oocytes. We stored the oocytes 4–6 days after injection for use in experiments. We verified delivery of EGFP-tagged AmtB to a region near the plasma membrane using a 96-well plate reader (BMG Labtechnologies, Inc., Durham, NC) to assess whole-oocyte fluorescence (Toye et al. 2006).

Solutions—The nominally CO_2/HCO_3^--free ND96 solution contained (mM): 96 NaCl, 2 KCl, 1 $MgCl_2$, 1.8 $CaCl_2$, and 5 HEPES. We titrated the solution to pH 7.50 using NaOH. The osmolality of all solutions was 200 mosmol/kg H_2O. We made the solution containing 5 mM NH_3/NH_4^+ in ND96 by replacing 5 mM NaCl with 5 mM NH_4Cl. We made 0.5 mM NH_3/NH_4^+ in ND96 by diluting the 5 mM NH_3/NH_4^+ solution 1:10 with ND96 solution.

Electrophysiological Measurements

Chamber—Oocytes were placed in plastic perfusion chamber with a channel 3 mm wide × 30 mm long, and constantly superfused at a flow of 3 ml/min. Perfusing solutions were delivered from plastic syringes and Tygon tubing using syringe pumps (Harvard Apparatus, South Natick, MA). Switching between solutions was performed by pneumatically operated valves (Clippard Instrument Laboratory, Cincinnati, OH). All experiments were performed at room temperature (~ 22°C).

Measurement of Intracellular pH (pH_i)—Our approach was similar to that detailed previously (Toye et al. 2006; Lu et al. 2006; Parker et al. 2008). Briefly, we impaled the oocyte with two microelectrodes, one for measuring membrane potential (connected to a model 725 two-electrode oocyte voltage-clamp amplifier; Warner Instruments Corp., Hamden, CT) and the other for measuring pH_i (connected to a model FD223 high-impedance electrometer; World Precision Instruments, Sarasota, FL). Both electrodes had tip diameters of ~ 1 μm. The pH microelectrode was of the liquid membrane style (proton cocktail no. 95293; Fluka Chemical Corp., Ronkonkoma, NY). The analog subtraction of the V_m-electrode signal from the pH-electrode signal produced the voltage due to pH_i. We acquired and analyzed data by computer, using software written in-house. We calibrated the pH_i/V_m in the chamber with pH standards at pH 6.0 and 8.0 (to determine the slope), followed by a single-point calibration with the standard ND96 solution (pH 7.50) in the chamber with the oocyte present, just before impalement. The mean spontaneous initial V_m in this study was −39 ± 2 mV (n = 30).

Measurement of Surface pH (pH_S)—The microelectrode for measuring pH_S (connected to a FD223 electrometer; World Precision Instruments) had a tip diameter of 15 μm and was of the same liquid-membrane design as the pH_i microelectrode. The external reference electrode for the V_m and pH_S measurements was a calomel half-cell (connected to a model 750 electrometer; World Precision Instruments) contacting a 3 M KCl-filled micropipette, which in turn contacted the fluid in the chamber. The analog subtraction of the calomel-electrode signal from the pH_S-electrode signal produced the signal due to pH_S. The analog subtraction of the calomel-electrode signal from the V_m-electrode signal produced the signal due to V_m. The voltage-clamp amplifier generated the virtual ground via a Ag/AgCl half cell (connected to the I_{Sense} input) contacting a second 3 M KCl-filled micro-electrode, the tip of which we positioned close to the oocyte. We used an ultrafine micromanipulator (model MPC-200 system; Sutter Instrument Co., Novato, CA) to position the pH_S-electrode tip at the surface of the oocyte, and then to advance it ~ 40 μm further, whereupon we observed a slight dimple in the membrane. Periodically, we withdrew the electrode 300 μm from the surface of

the oocyte for recalibration in the bulk extracellular fluid (pH 7.50). The fluid bathing the oocyte flowed at 3 ml/min. Relative to the flowing solution, the tip of the pH_S microelectrode was just in the "shadow" of the oocyte (Fig. 1).

Analysis of pH Data

Initial dpH_i/dt—We computed the initial rate of change of pH_i (dpH_i/dt)— produced by introducing 5 mM NH_3/NH_4^+—by determining the line of best fit to the steepest part of the pH_i vs. time record.

Maximum pH_S Spike Heights—We used the following approach to compute the maximum magnitude (i.e., "spike height" or ΔpH_S) of the pH_S transient elicited by applying 5 or 0.5 mM extracellular NH_3/NH_4^+. We determined the initial pH_S—that is, before application of NH_3/NH_4^+—by comparing the pH_S-electrode voltage signal when the electrode tip was at the oocyte surface with the voltage signal obtained when the tip was in the bulk extracellular fluid (assumed pH = 7.50). We determined the maximum pH_S during the NH_3/NH_4^+ exposure by comparing the voltage signal (at a time corresponding to the extreme pH_S value) when the electrode tip was at the oocyte surface with the voltage signal obtained a few minutes later, when the tip was in the bulk extracellular fluid (assumed pH = 7.50). The ΔpH_S was the algebraic difference between the extreme and the initial pH values, one based on a calibration in an ordinary ND96 solution and the other based on a separate calibration in the NH_3/NH_4^+-containing solution. We performed separate calibrations of the pH_S electrode in the plain and NH_3/NH_4^+-containing ND96 solutions to minimize potential errors in the event that NH_3/NH_4^+ affects the proton cocktail.

NMR Spectroscopy

Measurements of Metabolites with ^1H-[^{13}C]NMR—Twenty oocytes were incubated with 0.5 mM $^{15}NH_3/^{15}NH_4^+$, washed extensively, and homogenized with ethanol to extract water-soluble metabolites. A small quantity of [2-^{13}C]glycine (30 nmol) was added as an internal concentration reference and to control for potential sample losses during the extraction procedure. After centrifugation of the homogenate, the supernatant was lyophilized and resuspended in 10% D_2O buffer containing a small amount of 3-(trimethylsilyl)-[2,2,3,3-d_4]-propionate(Na^+) (TSP) as a chemical-shift reference. ^1H-[^{13}C]NMR spectra were acquired fully relaxed at 11.7 T (Patel et al. 2005), using a high-resolution Bruker Avance NMR spectrometer operating at 500.13 MHz (^1H) and 125.7 MHz (^{13}C). Spectral data were acquired fully relaxed with a sweep width of 6009 Hz, 8192 data points, interscan delay of 20 s, and 128 scans. Free-induction decays were zero filled, exponential filtered (LB = 0.5 Hz), and Fourier transformed. Metabolite peak intensities were measured by integration and referenced to ^{13}C-labeled glycine with correction for differences in the number of hydrogen atoms. The glycine signal was determined to be 100% enriched with ^{13}C, indicating no significant overlap with endogenous signals.

Measurements of $^{15}NH_3/^{15}NH_4^+$ with ^1H-^{15}N HSQC—Eighty oocytes were incubated with $^{15}NH_3/^{15}NH_4^+$ for 30 min, followed by extensive washing with ^{15}N-free/NH_3/NH_4^+-free buffer. The washed oocytes were cooled on ice and homogenized, yielding ~0.4 ml of supernatant after centrifugation. The medium was then acidified with 50 μl of 2.5 M HCl, 50 μl of D_2O was added for field-frequency lock, and samples were loaded into 5-mm NMR tubes. NMR spectra were obtained at 5°C to minimize the exchange of hydrogen atoms between ammonia and water. NMR experiments were performed at 11.7 T using a high-resolution Bruker Avance NMR spectrometer operating at 500.13 MHz (^1H) and 50.683 MHz (^{15}N). Measurements of total $^{15}NH_3/^{15}NH_4^+$ concentrations in oocytes were determined with the Heteronuclear (^1H-^{15}N) Single Quantum Coherence (HSQC) NMR spectroscopy technique (Grzesiek and Bax 1993; Kanamori et al. 1995). HSQC is well suited for detection of nuclei

(e.g., ^{15}N) with a low gyromagnetic ratio (γ). Because γ for ^{15}N is ~10 times lower than for ^{1}H, the sensitivity for ammonia-nitrogen detection is enhanced by a factor of $(\gamma_H/\gamma_N)^{5/2} \approx 306$. Water suppression was achieved using the Water Suppression by Gradient-Tailored Excitation (WATERGATE) technique (Piotto et al. 1992). ^{15}N decoupling was obtained using Waltz16 (Shaka et al. 1983). Free-induction decays were acquired with a spectral width of 6009 Hz, 8192 data points, interscan interval of 10 s, and 128 scans. All spectra were zero filled to 65,536 points. The total ammonium ($NH_3 + NH_4^+$) concentrations in oocytes were determined by comparing the integrated intensities of the ammonia ^{1}H resonance to the incubation medium containing 0.5 mM $^{15}NH_3/^{15}NH_4^+$, using the same pulse acquisition conditions, and assuming that oocytes are spheres of 1.2-mm diameter and contain 40% water by weight. ^{1}H-^{15}N HSQC spectra of oocytes and their incubation medium were acquired in a paired manner.

Statistics

We present data as mean ± SE. To compare the difference between two means, we performed a Student's *t*-test (two tails). To compare more than two means, we performed a one-way ANOVA and a Student-Newman-Keuls (SNK) multiple comparison, using KaleidaGraph (Version 4; Synergy Software). We considered $p < 0.05$ to be significant.

Results

Figure 1 summarizes how the influx of NH_3 would affect pH_S. As NH_3 enters the cell, $[NH_3]$ near the external surface of the membrane—$[NH_3]_S$—falls. The replenishment of the lost NH_3 near membrane surface occurs by two routes. First, NH_3 diffuses from the bulk extracellular fluid to approach the membrane, an effect that we cannot detect. Second, NH_4^+ near the membrane dissociates to form both NH_3 as well as the H^+ that we detect as a fall in pH_S. As the concentration of NH_3 inside the cell ($[NH_3]_i$) rises, the influx of NH_3 slows, and pH_S relaxes toward the pH of the bulk extracellular fluid (pH_{Bulk}). In Fig. 1, we assume that only NH_3 enters the cell. If only NH_4^+ enters, the reverse set of events would occur and pH_S would rise. In the Discussion, we consider the situation in which both NH_3 and NH_4^+ enter.

We explored the model in Fig. 1 by exposing oocytes to 5 or 0.5 mM NH_3/NH_4^+. Figures 2 and 3 show representative experiments at these two levels of NH_3/NH_4^+, and Fig. 4 summarizes the mean values for these experiments.

Effects of 5 mM NH_3/NH_4^+

Figure 2 shows the results of representative experiments on oocytes exposed to a relatively high level of NH_3/NH_4^+, 5 mM.

H_2O-Injected Control oocyte—Figure 2a refers to a control, H_2O-injected oocyte. Here — as previously reported by others for 20 mM NH_3/NH_4^+ (Burckhardt and Frömter 1992; Keicher and Meech 1994)—the addition of 5 mM NH_3/NH_4^+ to the extracellular fluid causes a moderately slow but sustained fall in pH_i. Simultaneously, pH_S abruptly falls by ~0.2 and then slowly decays (i.e., rises toward pH_{Bulk}). The initial fall in pH_S indicates that the influx of NH_3 (as opposed to NH_4^+) is dominant with respect to effects on pH_S. Note that, at a time when pH_i has reached a stable value, pH_S is still substantially lower than pH_{Bulk}, indicating that NH_3 is still entering the cell. Applying 5 mM NH_3/NH_4^+ also causes a very slowly developing depolarization that reaches a peak after nearly 15 min—not the instantaneous depolarization expected of a pre-existing NH_4^+ channel—that slowly decays by nearly 9 mV.

The removal of the NH_3/NH_4^+ leads to a slow recovery of pH_i that is incomplete over the time frame of this experiment. The removal of NH_3/NH_4^+ causes pH_S to overshoot pH_{Bulk} by a

small amount (0.048 ± 0.004; $n = 5$), and then to decay slowly. The presence of an overshoot implies that—regarding effects on pH_S—a small efflux of NH_3 dominates over any efflux of NH_4^+. This exiting NH_3 presumably arises from a small amount of intracellular NH_4^+ that dissociated to form H^+ (which would lower pH_i) and NH_3 (which would exit the cell). The short duration of the overshoot implies that the efflux was of short duration (i.e., that the pool of intracellular NH_4^+ was small). If intracellular NH_4^+ had accumulated to a substantial degree during the NH_3/NH_4^+exposure, then the removal of NH_3/NH_4^+ should have led to an abrupt fall in pH_i (which we did not observe) and a pH_S overshoot whose magnitude should have matched that of the initial NH_3/NH_4^+-induced fall in pH_S (i.e., ~0.2). Removing NH_3/NH_4^+ also causes V_m to undershoot its initial level by ~1 mV and then to relax to the pre- NH_3/NH_4^+ value. Note that the speed of the repolarization during NH_3/NH_4^+ removal is much faster than the depolarization during NH_3/NH_4^+ application, but still slower than the speed of the pH_S increase during NH_3/NH_4^+ removal.

Oocyte Expressing AmtB Tagged with EGFP—Figure 2b shows two experiments on oocytes expressing AmtB-EGFP. At the left, the switch to 5 mM NH_3/NH_4^+ causes a fall in pH_i, though one that is slower than for the H_2O oocyte. On the other hand, the maximal fall in surface pH (which we refer to as $-\Delta pH_S$) is substantially larger for the AmtB-EGFP oocyte than for the H_2O-injected oocyte, implying that the relative uptake of NH_3 over NH_4^+ is higher in the AmtB oocyte. In the oocyte at the left in Fig. 2b, this shift in pH_S at first decays rapidly and then more slowly. In the oocyte at the right in Fig. 2b, the fall in pH_S decays very slowly throughout the NH_3/NH_4^+ exposure. In both AmtB oocytes—as was true for the H_2O oocyte —pH_S fails to decay fully to pH_{Bulk} during the NH_3/NH_4^+ exposure. The V_m changes induced by application and removal of NH_3/NH_4^+ are similar to, but smaller than, those for H_2O oocytes.

The removal of NH_3/NH_4^+ produces about the same effects in the AmtB oocyte as in the H_2O oocyte (mean overshoot in AmtB oocytes, 0.037 ± 0.004; $n = 6$).

Summary of AmtB-EGFP Versus H_2O—As summarized on the left side in Fig. 4 for a larger number of experiments, the effect of AmtB vs. H_2O is statistically significant for the initial rate of pH_i decrease (dpH_i/dt) elicited by NH_3/NH_4^+ (Fig. 4a). The slower fall of pH_i in the case of AmtB oocytes is consistent with the hypothesis that, regarding effects on pH_i (a) AmtB acts by predominantly enhancing NH_3 vs. NH_4^+ influx (b) the enhanced influx of NH_3 to some extent promotes the reaction $NH_3 + H^+ \rightarrow NH_4^+$ in the cytosol, and (c) the consumption of cytosolic H^+ slows the NH_3/NH_4^+-induced fall in pH_i.

The effect of expressing AmtB did not reach statistical significance regarding the NH_3/NH_4^+-induced ΔpH_i (Fig. 4b). However, AmtB oocytes had a greater $-\Delta pH_S$ (Fig. 4c), indicating a greater relative influx of NH_3 and thus supporting the hypothesis in the previous paragraph. Finally, the AmtB oocytes had a smaller ΔV_m (Fig. 4d).

Effects of 0.5 mM NH_3/NH_4^+

Figure 3 shows representative data from a pair of oocytes exposed to a relatively low level of NH_3/NH_4^+, 0.5 mM.

H_2O-Injected Control Oocyte—As shown in Fig. 3a for a H_2O-injected oocyte, the switch to 0.5 mM NH_3/NH_4^+ causes a slow and very slight fall in pH_i. Although pH_S abruptly falls, $-\Delta pH_S$ is substantially lower than for H_2O oocytes exposed to the much higher level of NH_3/NH_4^+ (i.e., 5 mM; see Fig. 2a). Nevertheless, regarding effects on pH_S, the effect of NH_3 influx (over NH_4^+ influx) is clearly dominant. The V_m changes caused by application and removal

of 0.5 mM NH_3/NH_4^+ are much smaller than those in the experiments with 5 mM NH_3/NH_4^+.

The removal of NH_3/NH_4^+ evoked virtually no recovery of pH_i in Fig. 3a, although some oocytes exhibited a slight pH_i recovery. In Fig. 3a, pH_S rose to a value ~0.02 higher than pH_{Bulk}. The mean pH_S overshoot was 0.006 ± 0.003 (n = 8; 0.006 vs. 0; p = 0.28). These data indicate that— regarding effects on pH_S—the efflux of NH_3 is negligible relative to that of NH_4^+.

Oocyte Expressing AmtB Tagged with EGFP—Figure 3b shows that, with an oocyte expressing AmtB-EGFP, the switch to 0.5 mM NH_3/NH_4^+ causes little change in pH_i. The maximal fall in pH_S is much larger for the AmtB-EGFP oocyte than for the H_2O oocyte, though both values are much smaller than for their counterparts in exposures to 5 mM NH_3/NH_4^+. The V_m change is minimal.

The removal of NH_3/NH_4^+ from AmtB-EGFP oocytes (Fig. 3b) evoked virtually the same response as in H_2O oocytes. The mean pH_S overshoot was 0.014 ± 0.006 (n = 8; 0.014 vs. 0; p = 0.30), indicating that—regarding effects on pH_S—the efflux of NH_3 is negligible relative to that of NH_4^+.

Summary of AmtB-EGFP Versus H_2O—As summarized on the right side in Fig. 4, the effect of AmtB vs. H_2O for an exposure to 0.5 mM NH_3/NH_4^+ follows essentially the same pattern as for an exposure to 5 mM, except that the difference for AmtB vs. H_2O is not statistically significant for dpH_i/dt (Fig. 4e). The dpH_i/dt for H_2O oocytes is significantly different from zero (p = 0.05) but not for AmtB oocytes (p = 0.26). As summarized in Fig. 4f, the ΔpH_i was not different from zero for H_2O oocytes (0.038 ± 0.010; n = 8; p = 0.15) but was significantly—but not substantially different—for AmtB oocytes (0.040 ± 0.005; n = 8; p = 0.01). As was the case for the exposures to 5 mM NH_3/NH_4^+, the AmtB oocytes also had a higher $-\Delta pH_S$ (Fig. 4g), indicating a greater relative NH_3 influx. As also was the case for the 5 mM exposures, the ΔV_m was lower for the AmtB oocytes (Fig. 4h).

Comparing ΔpH_S data for 5 mM vs. 0.5 mM (Fig. 4c vs. g), we see that the difference (always higher for the experiments with 5 mM NH_3/NH_4^+) is statistically significant both for H_2O oocytes and for AmtB oocytes.

NMR Studies of Oocytes Exposed to ^{15}N-Labeled 0.5 mM NH_3/NH_4^+

A paradox in our results is that AmtB increases $-\Delta pH_S$ (Fig. 4g)—indicating that AmtB enhances the influx of NH_3—and yet has no significant effect on the initial dpH_i/dt (Fig. 4e) or ΔpH_i (Fig. 4f). Moreover, removing extra-cellular 0.5 mM NH_3/NH_4^+ produces little pH_S overshoot beyond pH_{Bulk} (Fig. 3a, b), indicating little efflux of NH_3. The most straightforward explanation for these data is that the oocyte somehow disposes of most incoming NH_3 by either metabolizing it to a neutral product or sequestering it. We test this hypothesis in the next two sections. Note that, a priori, we can rule out the possibility that the oocyte metabolizes or sequesters NH_4^+ (as opposed to NH_3). If the oocyte first converted the entering NH_3 to NH_4^+ ($NH_3 + H^+ \rightarrow NH_4^+$) and then metabolized that NH_4^+ to a neutral product(s), the result would be an increase in pH_i, which we would have easily observed in experiments with 0.5 mM NH_3/NH_4^+.

Assessment of Glutamine Formation—The leading candidate for the metabolism of NH_3 to a neutral product would be the conversion of glutamate to glutamine via glutamine synthetase: $Glu^- + MgATP^= + NH_3 \rightarrow Gln + MgADP^- + H_2PO_4^-$.

To test this hypothesis, we incubated noninjected oocytes for 10 min either in ND96 alone (for sham incubation) or in ND96 plus 0.5 mM $^{15}NH_3/^{15}NH_4^+$. We then homogenized the oocytes with ethanol to extract water-soluble metabolites and subjected the extract to ^1H-[^{13}C] NMR spectroscopy (Fig. 5). The extract from oocytes incubated in $^{15}NH_3/^{15}NH_4^+$ exhibited a very low Gln signal ([Gln] ≅ 1.1 mM) vs. the shams (undetectable Gln). RhAG, a component of the erythrocyte Rh complex, has a higher NH_3/CO_2 permeability ratio than AmtB (Endeward et al. 2006;Musa-Aziz et al. 2009), and RhAG-expressing oocytes (like AmtB oocytes) exhibit high ΔpH_S values and very small pH_i changes when exposed to 0.5 mM NH_3/NH_4^+. However, extracts from RhAG oocytes exposed to 0.5 mM $^{15}NH_3/^{15}NH_4^+$ have undetectable Gln (not shown).

^1H-^{15}N-HSQC spectra (acquired as in Fig. 6 from a separate batch of RhAG oocytes incubated with 0.5 mM $^{15}NH_4Cl$) showed no significant ^{15}N-enrichment of amides in the metabolites, although we only examined Gln and a few other likely metabolites. Although we cannot rule out the possibility that oocytes sequester NH_3 via unknown metabolic pathways, our ^1H-[^{13}C] NMR and ^1H-^{15}N-HSQC data rule out substantial conversion of NH_3 to Gln and provide no evidence for other pathways.

NH_3/NH_4^+ *Accumulation in Oocyte Water*

To determine if oocytes accumulate NH_3/NH_4^+ per se, we incubated noninjected control oocytes or AmtB oocytes in ND96 containing 0.5 mM $^{15}NH_3/^{15}NH_4^+$ for 30 min. After the incubation, we washed the oocytes with a NH_3-free ND96 solution and, following homogenization and centrifugation, measured the total $15NH_3 + NH_4^+$ of the supernatant using ^1H-^{15}N HSQC (Fig. 6a, b). We found that $^{15}NH_3/^{15}NH_4^+$—which reflects only NH_3/NH_4^+ taken up during the incubation—was ~30% higher in AmtB oocytes (4.15 mM computed for total oocyte H_2O) than in control noninjected oocytes (3.33 mM). Because pH_i was ~7.40 in these experiments—and pH_o was 7.50 and $[NH_3/NH_4^+]_o$ was 0.5 mM—we can conclude that if NH_3 fully equilibrated across the cell membrane, cytosolic $[NH_3/NH_4^+]$ (i.e., the concentration in the water in direct contact with the inner surface of the plasma membrane) could only have been 0.5 mM × $10^{(7.50-7.40)}$ ≅ 0.6 mM. Note that even this level of cytosolic NH_3/NH_4^+ would have led—upon the removal of extracellular NH_3/NH_4^+—to a substantial fall in pH_i and a large transient overshoot of pH_S, neither of which we observed. Thus, we conclude that cytosolic $[NH_3/NH_4^+]$ must have been substantially lower than 0.6 mM. The most straightforward explanation for the extremely high level of intracellular NH_3/NH_4^+ that we actually observed in the NMR experiments (i.e., for the $3^+ - 4^+$ mM) is that the vast majority of intracellular NH_3/NH_4^+ was, in fact, confined to an acidic intracellular compartment.

Discussion

Overview

The pH_i data in the present paper confirm the earlier observation that an exposure of a control *Xenopus* oocyte (i.e., not heterologously expressing other proteins) to a relatively high level of NH_3/NH_4^+ leads to a paradoxical intracellular acidification (Burckhardt and Frömter 1992; Keicher and Meech 1994). Earlier investigators had also found that an exposure to a relatively low level of NH_3/NH_4^+ leads to a negligible pH_i change (Bakouh et al. 2004). We now confirm both observations in H_2O oocytes (Fig. 4b and f, respectively). In addition, we make the novel observation that the expression of AmtB slows the pH_i fall elicited by an exposure to 5 mM NH_3/NH_4^+ (Fig. 4a), consistent with the hypothesis that AmtB predominantly promotes the influx of NH_3 over NH_4^+ (regarding effects on pH_i). However, we believe that the most important contributions of the present study are (a) the simultaneous application of pH_S and pH_i measurements, which provide new insights into how *Xenopus*

oocytes handle exposures to NH_3/NH_4^+, and (b) novel pH_S data that show that AmtB enhances NH_3 fluxes during exposures to both 5 mM and 0.5 mM NH_3/NH_4^+.

Evidence for Unusual NH_3/NH_4^+ Handling by *Xenopus* Oocytes

Regardless of whether the concentration is 5 or 0.5 mM, exposing an oocyte to NH_3/NH_4^+ causes an initial pH_S decrease, the explanation for which is straightforward: the influx of NH_3 causes a depletion of NH_3 at the extracellular surface of the oocyte, leading to the reaction $NH_4^+ \rightarrow NH_3 + H^+$. However, five other observations indicate that the handling of NH_3 by *Xenopus* oocytes is unusual compared to that by other cells studied thus far.

First, when one exposes an oocyte to a relatively high level of NH_3/NH_4^+, pH_i paradoxically falls. Almost all other cells—the exceptions being membranes that mediate either a massive influx of NH_4^+ (Aickin and Thomas 1977; Kikeri et al. 1989) or no apparent flux of either NH_3 or NH_4^+ (Waisbren et al. 1994; Singh et al. 1995)—exhibit a rapid pH_i increase, due to the influx and protonation of NH_3 (Roos and Boron 1981). Working on oocytes, previous investigators had observed NH_3/NH_4^+-induced pH_i decreases when introducing 10–20 mM NH_3/NH_4^+ (Burckhardt and Frömter 1992; Keicher and Meech 1994; Bakouh et al. 2006). In the present paper, we observed similar, though smaller pH_i decreases—with both H_2O-injected controls and AmtB oocytes—when introducing 5 mM NH_3/NH_4^+ (Fig. 2). This paradoxical fall in pH_i implies that the rate of intracellular acid loading is higher than that of acid extrusion. We examine potential explanations below, under "Models of NH_3/NH_4^+ Handling by *Xenopus* Oocytes: 'High' $[NH_3/NH_4^+]_o$."

Second, when one exposes an oocyte to a relatively low level (e.g., 0.5 mM) of NH_3/NH_4^+, pH_i either falls very slowly, and by a small amount (Figs. 3, 4e, f; H_2O bars), or does not change significantly (Fig. 4e, f; AmtB bars). These observations on H_2O oocytes confirm earlier work (Bakouh et al. 2004,2006).

Third, after an exposure to relatively high levels of NH_3/NH_4^+—10 to 20 mM in the case of others (Burckhardt and Frömter 1992; Keicher and Meech 1994; Bakouh et al. 2004, 2006) or 5 mM in the present work (Fig. 2)—the removal of extracellular NH_3/NH_4^+ causes pH_i to increase slowly, rather than to decrease rapidly (due to NH_3 efflux followed by the intracellular reaction $NH_4^+ \rightarrow NH_3 + H^+$), as has been observed by numerous investigators working on most other cell types.

Fourth, although introducing NH_3/NH_4^+ produces an abrupt fall in pH_S—indicative of NH_3 influx—the subsequent decay in pH_S is generally very slow, regardless of whether the oocytes are exposed to 5 or 0.5 mM NH_3/NH_4^+. In H_2O-injected oocytes (Figs. 2a, 3a), the decay is monotonic and extremely slow throughout. In AmtB oocytes, the decay in pH_S is sometimes fast at first, but then extremely slow (see Fig. 2b, left, and Fig. 3b). In some other experiments on AmtB oocytes, even this rapid phase of pH_S decay is absent (Fig. 2b, right). In neither case does pH_S return to the pH_{Bulk} value of 7.50 during the course of an NH_3/NH_4^+ exposure lasting ~15 min or more. Thus, the decay in pH_S in these experiments with NH_3 is decidedly slower than the rapid decay in pH_S in oocytes exposed to CO_2 (Endeward et al. 2006)—a decay that is complete in ~5 min. These observations are consistent with the hypothesis that—unlike CO_2 (which equilibrates across the membrane in a few minutes)—NH_3 is still far from equilibrated across the plasma membrane and continues to enter the oocyte for a prolonged period (Figs. 2, 3). A corollary is that the oocyte somehow maintains a relatively low level of NH_3 near the inner surface of the cell membrane.

Fifth, although one would expect that removing extracellular NH_3/NH_4^+ would cause pH_S to increase abruptly and overshoot the initial pH_S (i.e., near the pH_{Bulk} of 7.50)—by an amount that approximates the magnitude of the pH_S decay during the preceding NH_3/NH_4^+ exposure

—in fact we observe little or no pH_S overshoot (Figs. 2, 3). Moreover, the expression of AmtB (vs. the injection of H_2O) increases the magnitudes of the rapid pH_S changes but does not produce a larger overshoot. These results imply that the NH_3 efflux from the oocyte is small, consistent with the hypothesis that (1) the pathways for NH_3 movement across the oocyte membrane are highly rectified (i.e., favoring influx over efflux), or (2) very little NH_4^+ is present in the cytosol near the plasma membrane at the end of an NH_3/NH_4^+ exposure. Thus, upon removal of extracellular NH_3/NH_4^+, very little free, cytosolic NH_4^+ is available for the reaction $NH_4^+ \rightarrow H^+ + NH_3$. This reaction is necessary not only for the pH_i to fall, but also to generate the NH_3 that subsequently exits and produces the pH_S overshoot. Moreover, a limited cytosolic NH_4^+ would minimize the outwardly directed diffusion potential for NH_4^+, and minimize a rebound hyperpolarization upon removal of extracellular NH_3/NH_4^+. Because we know of no examples of a rectifying of a gas flux through either lipid or a protein channel, option 2 is the simplest explanation, and would account for the observations that removal of extracellular NH_3/NH_4^+ fails to cause (a) a fall in oocyte pH_i (b) a large pH_S overshoot, and (c) a rebound hyperpolarization. Instead, NH_3/NH_4^+ removal merely eliminates the processes that cause pH_S to fall and V_m to become more positive, causing these parameters simply to return to their pre-NH_3/NH_4^+ values.

Models of NH_3/NH_4^+ Handling by *Xenopus* Oocytes: "Low" $[NH_3/NH_4^+]_o$

In the section following this one, we consider potential explanations for the pH_i and pH_S data obtained with the exposure to and withdrawal of relatively high NH_3/NH_4^+ levels (e.g., 5 mM), with their attendant large and paradoxical pH_i changes. In this section, we examine experiments with relatively low NH_3/NH_4^+ levels (e.g., 0.5 mM), where the paradoxical pH_i changes—mediated by a process with a low affinity for NH_3 and/or NH_4^+—are minimal. We consider five models of NH_3 handling by *Xenopus* oocytes (Fig. 7) that could account for why an exposure to NH_3/NH_4^+ would cause virtually no change in pH_i.

Model A: Is the pH_i Effect of NH_3 Influx Perfectly Matched by the pH_i Effect of NH_4^+ Influx (Fig. 7a)—In order for the influxes of NH_3 and NH_4^+ to cause no change in pH_i, the influx of NH_3 (J_{NH_3}) and the influx of NH_4^+ ($J_{NH_4^+}$) would have to be in the ratio $10^{(pHi-pKa)}$, where pH_i is the initial pH_i and pK_a refers to the intracellular equilibrium $NH_4^+ \rightleftarrows NH_3+H^+$. To make this point more clearly, we imagine that the oocyte's cytosol contains a tiny amount of NH_3/NH_4^+ that is equilibrated at the initial pH_i. If we assume that the pK_a of this reaction is 9.2, and, for the sake of simplicity, that the pH_i is 7.2, then

$$\frac{[NH_3]_i}{[NH_4^+]_i} = 10^{pH_i - pK_a} = 10^{7.2-9.2} = \frac{1}{100} \quad (1)$$

Thus, if $J_{NH_3}/J_{NH_4^+}$ also were 1/100, then the parallel influxes of NH_3 and NH_4^+ would not disturb the ratio $[NH_3]_i/[NH_4^+]_i$ and hence would not disturb the NH_3/NH_4^+ equilibrium or pH_i. (In Fig. 7a, we assume an NH_3 influx of 100 arbitrary units.) We now define the virtual $J_{NH_3}/J_{NH_4^+}$ ratio that would produce no change in the actual pH_i:

$$\left(\frac{J_{NH_3}}{J_{NH_4^+}}\right)_{Null} \equiv \frac{[NH_3]_i}{[NH_4^+]_i} = 10^{pH_i - pK_a} \quad (2)$$

In our example $(J_{NH_3}/J_{NH_4^+})_{Null}$ is 1/100. To be more general, we can define $(J_{NH_3}/J_{NH_4^+})_{Null}$ in terms of the pH on either side of the membrane:

$$\left(\frac{J_{NH_3}}{J_{NH_4^+}}\right)_{Null} \equiv \frac{[NH_3]_i}{[NH_4^+]_i} = 10^{pH-pK_a} \quad (3)$$

Because solutions on opposite sides of the membrane will generally have different pH values, they will also have different requirements for $(J_{NH_3}/J_{NH_4^+})_{Null}$, which—as we see below—can have interesting consequences.

We can also define the virtual value of pH that—given the actual fluxes of NH_3 and NH_4^+—would produce no pH change in the compartment under consideration. Starting with an expression analogous to Eq. 3 and solving for pH, we have

$$pH_{Null} = pK_a + \log\frac{J_{NH_3}}{J_{NH_4^+}} \quad (4)$$

This equation has the form of the familiar Henderson-Hasselbalch equation, except that here we replace concentrations with fluxes. If the $J_{NH_3}/J_{NH_4^+}$ ratio were 1/100 and pK_a were 9.2, then pH_{Null} would be

$$pH_{Null} = 9.2 + \log\frac{1}{100} = 7.2 \quad (5)$$

If the actual pH_i were 7.2 (i.e., the same as pH_{Null} in this example), the NH_3/NH_4^+ fluxes would not alter pH_i. However, because the pH of the bulk extracellular fluid is 7.5, this same $J_{NH_3}/J_{NH_4^+}$ ratio of 1/100 would necessarily alter pH_S. To determine the direction of the effect on pH_S, we return to Eq. 3. For the NH_3/NH_4^+ fluxes to produce no change in pH_S (where the initial $pH_S = pH_{Bulk} = 7.50$),

$$\left(\frac{J_{NH_3}}{J_{NH_4^+}}\right)_{Null} = 10^{(pH_{Bulk}-pK_a)} = 10^{(7.5-9.2)} = \frac{1}{50} = \frac{2}{100} \quad (6)$$

To produce the observed decrease in pH_S, as in Fig. 1, the fluxes would have to be in a ratio >1/50 (or 2/100). However, if $J_{NH_3}/J_{NH_4^+}$ were only 1/100—the value necessary to stabilize pH_i—the influx of NH_3 would be too low (or the influx of NH_4^+ would be too high) to stabilize pH_S, and the following reaction on the extracellular surface of the oocyte would replenish some of the lost NH_4^+: $NH_3 + H^+ + NH_4^+$ (Fig. 7a). Thus, if the $J_{NH_3}/J_{NH_4^+}$ ratio were positioned to stabilize pH_i, pH_S would rise, rather than fall as actually observed. Obviously, $J_{NH_3}/J_{NH_4^+}$ cannot simultaneously be 1/100 (to explain the stability of pH_i) and >2/100 (to explain the fall in pH_S). Therefore, no combination of NH_3 influx and NH_4^+ influx—regardless of mechanism (e.g., influx through a Na/K/Cl cotransporter or a channel)—can simultaneously account, by itself, for the pH_i and pH_S data. Thus, we can rule out model A for experiments at 0.5 mM NH_3/NH_4^+. Below, we see that a similar line of reasoning rules out NH_4^+ influx as a potential mechanism for the paradoxical fall of pH_i in 5 mM NH_3/NH_4^+.

Table 1 summarizes the directions of the expected pH changes for the three possible conditions: $pH < pH_{Null}$, $pH = pH_{Null}$, and $pH > pH_{Null}$.[1] These pH vs. pH_{Null} relationships are mirrored by corresponding $J_{NH_3}/J_{NH_4^+}$ vs. $(J_{NH_3}/J_{NH_4^+})_{Null}$ relationships. Notice that, in the case of

inequalities, the directions of the pH changes are opposite on the side from which the NH_3 and NH_4^+ exit vs. the side which NH_3 and NH_4^+ enter.

Note that the model that we developed here only allows us to conclude that a NH_3/NH_4^+-induced fall in pH_S in our experiments is associated with a J_{NH3}/J_{NH4^+} that is >1/50. We cannot rule out an influx of NH_4^+. In fact, a hypothetical influx of NH_4^+ could be 49-fold greater than the influx of NH_3, and yet pH_S still would fall. On the other hand, a large absolute influx of NH_4^+ would slow the fall in pH_S and reduce the magnitude of $-pH_S$. Such kinetic issues can only be addressed by a model that computes the time course of pH_S.

Model B: Is the Influx of NH_3 Perfectly Matched by an Influx of H^+ (Fig. 7b)—Even if NH_4^+ did not enter the oocyte, pH_i would be stable if J_{NH3} were matched by a comparable J_{H+}. Each entering NH_3 would undergo the reaction $NH_3 + H^+ \rightarrow NH_4^+$, and the lost cytosolic H^+ would be replenished by an influx of H^+. In Fig. 7b, we assume a J_{H+} of 100 arbitrary units and a J_{NH3} of 100, and we also assume that the NH_3 disappearing from the extracellular surface of the cell would be replenished by an NH_3 diffusion from the bulk extracellular fluid (ECF) of 90 and a contribution of 10 from the extracellular reaction $NH_4^+ \rightarrow H^+ + NH_3$. Because this model results in a net consumption of H^+ at the extracellular surface (100 – 10 = 90 in this example), pH_S would rise rather than fall as we observe. Moreover, this model would predict an enormous production of intracellular NH_4^+, which would produce cell swelling; we observe no tendency for the oocyte to swell. Finally, the massive accumulation of intracellular NH_4^+ would, upon removal of extracellular NH_3/NH_4^+, lead to a substantial decline in pH_i and overshoot of pH_S (i.e., increase beyond the pH_{Bulk} value of 7.50), neither of which we observe. In this analysis, we have assumed no flux of NH_4^+. To the extent that NH_4^+ entered the oocyte, we would require less H^+ influx to produce no pH_i change. However, any substantial H^+ influx would be inconsistent with our pH_S data, and we have already seen in our analysis of model A that NH_4^+ influx cannot account for our data. It is theoretically possible that the oocyte could export NH_4^+, thereby avoiding swelling. However, the electrochemical gradient for NH_4^+ is inward, and in any case pH_S would rise (rather than fall, as we observe). Therefore, model B is incorrect.

Model C: Is the Influx of NH_3 Perfectly Matched by the Metabolic Production of H^+ (Fig. 7c)—This analysis is similar to that for model B except that we can ignore the incorrect predictions that stem from H^+ influx across the plasma membrane. Nevertheless, we are left with the massive accumulation of intracellular NH_4^+, which would lead to cell swelling and—upon NH_3/NH_4^+ removal—a large pH_i decline and a large pH_S overshoot, neither of which we observe.

Model D: Is Virtually all Entering NH_3 Metabolized to a Neutral Product(s) (Fig. 7d)—If an amido-transferase reaction (e.g., the conversion of glutamate to glutamine) consumed the entering NH_3, pH_i would not change. Moreover, NH_4^+ would not accumulate inside the cell during the NH_3/NH_4^+ exposure. Thus following the withdrawal of extracellular NH_3/NH_4^+, pH_i would not fall and pH_S would not overshoot pH_{Bulk}. To test model D, we attempted to detect Gln by both ^1H-[^{13}C] (Fig. 5) and ^1H-^{15}N-HSQC NMR spectroscopy, but observed little Gln or other likely NH_3 metabolite. These data, combined with our demonstration of substantial NH_3/NH_4^+ accumulation (Fig. 6)—presumably in acidic intracellular vesicles—make it unlikely that the oocyte performs substantial conversion of NH_3 by metabolic processes.

[1]In our analysis, we assume that NH_3 and NH_4^+ move in the same direction. If they should move in opposite directions, then pH would always fall on the side of the membrane toward which NH_4^+ moves, and would always rise on the opposite side.

Model E: Is Virtually all Entering NH_3 Sequestered in an Acidic Subcompartment as NH_4^+ (Fig. 7e)—In this model, a small fraction of entering NH_3 equilibrates with H^+ to produce NH_4^+ in a cytoplasmic microenvironment immediately below the surface of the plasma membrane. Both the NH_3 and the NH_4^+ would diffuse slightly deeper into the oocyte, where NH_3 enters an acidic vesicle and becomes trapped as NH_4^+. To test this hypothesis, we used ^1H-^{15}N HSQC NMR spectroscopy to measure total intercellular NH_3/NH_4^+, finding values (Fig. 6) that were far too high to represent cytosolic NH_3/NH_4^+. Thus, we conclude that the vast majority of intracellular NH_3/NH_4^+ must be trapped as NH_4^+ in vesicles. Indeed, oocytes contain copious yolk granules or platelets (50% of oocyte volume), containing yolk proteins (80% of total cell proteins), and having a pH of ~5.6 (Fagotto and Maxfield 1994a, 1994b;Fagotto 1995). By microscopy, a layer of vesicles begins within ~10 μm of the plasma membrane (Lu et al. 2006).

We predict that—at least during brief experiments such as ours—NH_3/NH_4^+ levels would rise only modestly in the small subcompartment between the membrane and the vesicles, and relatively little of the entering NH_3 could escape the aforementioned vesicles to penetrate deeper into the oocyte. The influx of NH_3 into the vesicle would lead to a fall in $[NH_3]$ at the vesicle surface, favoring the reaction $NH_4^+ \rightarrow NH_3 + H^+$, which would minimize pH_i changes. It is possible that a high intravesicular buffering power (provided by abundant yolk proteins) could, by itself, sufficiently stabilize intravesicular pH over the course of our experiments. In addition, vesicular H^+ pumps could replenish intravesicular H^+, with cytosolic metabolism providing the necessary H^+, again tending to stabilize cytosolic pH.

The NH_4^+-trapping hypothesis would account for all key, paradoxical findings dealing with NH_3. (1) The extracellular addition of 0.5 mM NH_3/NH_4^+ produces a pH_i change of virtually nil (the conversion of incoming NH_3 to NH_4^+ occurs in a subcompartment, not in the cytosol). (2) The fall in pH_S produced by the extracellular addition of NH_3/NH_4^+ relaxes very slowly (NH_3 continues to enter the subcompartment, and perhaps deeper into the oocyte, for many tens of minutes). (3) The extracellular removal of NH_3/NH_4^+ causes virtually no fall in pH_i (virtually no NH_4^+ is present in the cytosol). And (4) the extracellular removal of NH_3/NH_4^+ produces little or no overshoot of pH_S (because little NH_3/NH_4^+ is present free in the cytosol near the plasma membrane, the efflux of NH_3 is very low).

Models of NH_3/NH_4^+ Handling by *Xenopus* Oocytes: "High" $[NH_3/NH_4^+]_o$

Compared to the analysis of data from experiments with 0.5 mM NH_3/NH_4^+, that of data from experiments with 5 mM NH_3/NH_4^+ is complicated by the paradoxical fall in pH_i (Fig. 2), which creates the added paradox that pH falls on both sides of the membrane.

Model A: Does the Influx of NH_4^+ Cause the Paradoxical Fall in pH_i?—Previous investigators favored the hypothesis that the paradoxical fall in pH_i is due to the influx of NH_4^+—via either an Na/K/Cl cotransporter (Keicher and Meech 1994) or a nonselective cation channel (Burckhardt and Frömter 1992)—followed by the cytosolic reaction $NH_4^+ \rightarrow NH_3 + H^+$. The channel hypothesis, in particular, requires that the oocyte dispose of the newly formed NH_3—by either NH_3 efflux or intracellular NH_3 metabolism or sequestration. Our pH_S data (see Fig. 2) demonstrate a net movement of NH_3 into the cell, ruling out the first NH_3-disposal option. In the introductory section, we noted limitations of the Na/K/Cl-cotransporter hypothesis. Moreover, although we agree that a NH_4^+ conductance is a reasonable explanation for the depolarization triggered by the exposure to NH_3/NH_4^+, two arguments will lead us to conclude here that the hypothesized NH_4^+ entry via a nonselective cation channel is not a viable explanation for the paradoxical fall in pH_i. When we apply 5 mM NH_3/NH_4^+, the speed of the pH_i decrease (an index of the hypothesized NH_4^+ influx) is maximal early on and then gradually wanes as pH_i stabilizes (see Fig. 2). On the other hand, the positive shift in V_m is small early

on and slowly reaches a maximal value over nearly 15 min. Thus, if the depolarization is an index of permeability to NH_4^+, we conclude that the NH_4^+ conductance develops far too slowly to account for the decrease in pH_i[2].

Finally, using the same logic as we did for model A in the previous section (see Fig. 7a), we can conclude that it is impossible for the NH_3/NH_4^+-influx ratio to be—at the same time—low enough to cause pH_i to fall and yet high enough to cause pH_S to fall. For example, if pH_i is 7.2 and pKa is 9.2, then $(J_{NH_3}/J_{NH_4^+})_{Null}$ would be 1/100. Thus, for the influx of NH_4^+ to lower pH_i, $J_{NH_3}/J_{NH_4^+}$ would have to be <1/100. However, as we saw earlier, for the influxes of NH_3/NH_4^+ to lower pH_S $(J_{NH_3}/J_{NH_4^+})_{Null}$ would have to be >2/100. Because $(J_{NH_3}/J_{NH_4^+})_{Null}$ cannot simultaneously be <1/100 and >2/100, the influx of NH_4^+—regardless of mechanism—cannot account for the paradoxical fall in pH_i.

We might note that, at least in theory, it would be possible for the parallel influxes of NH_3 and NH_4^+ to cause both pH_i and pH_S to fall. As noted in Table 1, in the compartment that NH_3 and NH_4^+ enter, the pH would fall if pH >pH_{Null}. As we have just seen, a fall in pH_S from an initial value of 7.5 requires that $J_{NH_3}/J_{NH_4^+}$ be >2/100; let us assume a $J_{NH_3}/J_{NH_4^+}$ of 10/100. For this ratio, pH_{Null} would be 8.2. Thus, if the initial pH_i were >8.2, a $J_{NH_3}/J_{NH_4^+}$ of 10/100 would cause pH_i to fall along with pH_S. (Of course, because the actual initial pH_i is far less than 8.2, this explanation is not valid for our data.) Using similar logic, we could predict conditions in which the parallel influxes of NH_3 and NH_4^+ would raise both pH_i and pH_S.

Model B: Does the Influx of H^+ Causes the Paradoxical Fall in pH_i?—As noted in the previous section's model B, in our analysis of data for 0.5 mM NH_3/NH_4^+, even an H^+ influx sufficient to stabilize pH_i in the face of an NH_3 influx (see Fig. 7b) would lead to a rise—rather than the observed fall—in pH_S. Because an even greater H^+ influx would be needed to produce a net fall in pH_i—and such a greater H^+ influx would cause an even greater increase in pH_S—we can rule out the H^+-influx model.

Model C: Does the Intracellular Release or Production of H^+ Cause the Paradoxical Fall in pH_i?—As noted in the previous section's model C (see Fig. 7c), the intracellular generation of H^+—by itself—during the NH_3/NH_4^+ exposure would lead to NH_4^+ accumulation in the cytosol and thus cell swelling (not observed). During NH_3/NH_4^+ withdrawal, the accumulated NH_4^+ would dissociate to produce H^+ (we observed no fall in pH_i) and NH_3, which would exit the cell (we observed no substantial pH_S overshoot). However, if H^+ generation occurred in parallel with trapping—in acidic intracellular vesicles—of nearly all incoming NH_3, then cytosolic H^+ production would promote accumulation of NH_4^+ in vesicles rather than in the cytosol. Thus, this hybrid H^+-generation/vesicular NH_4^+-trapping model (see Fig. 7e) would account for our data with 5 mM NH_3/NH_4^+.

Model D: Does the Closing of NH_4^+-Permeable Channels Cause pH_i to Rise Following Withdrawal of High Levels of NH_3/NH_4^+?—The only explanation offered by previous investigators for the observed rise in pH_i with NH_3/NH_4^+ removal is that the sudden repolarization of the oocyte membrane would close nonselective cation channels and thus allow a slow efflux of accumulated cytosolic NH_4^+, leading to a sluggish pH_i recovery (Burckhardt and Frömter 1992). Presumably, the release of previously sequestered NH_3 would lead to the cytosolic reaction $NH_3 + H^+ \rightarrow NH_4^+$, which would lead to a slow rise in pH_i. One argument against the channel model is that, as already noted, our data[3] indicate that $[NH_4^+]$ in the cytosol near the inner surface of the plasma membrane must be very low, and thus NH_4^+ efflux could

[2]We cannot rule out the possibility that the NH_4^+ conductance is immediately high, but that other conductances—also initially high—gradually decline to allow V_m to approach $E_{NH_4^+}$.

[3]The removal of NH_3/NH_4^+ causes neither a fall in pH_i nor a rise in pH_S that substantially overshoots the initial value.

not produce a sustained pH_i increase. Consistent with this idea, following the removal of NH_3/NH_4^+, the V_m undershoot is small and short-lived (Fig. 2).[4] A much stronger argument flows from our new analysis of $(J_{NH_3}/J_{NH_4^+})_{Null}$ values. For a hypothetical efflux of NH_4^+ to cause a rise in pH_i—starting from an initial pH_i of, say, 6.9—the absolute value of $(J_{NH_3}/J_{NH_4^+})_{Null}$ would have to be $<[NH_3]_i/[NH_4^+]_i = 10^{(6.9-9.2)} = 0.5/100$ (see Eq. 3 and Table 1). On the other hand, even though pH_S does not exhibit a substantial overshoot of its initial value, the small pH_S overshoot that we do observe indicates that $|J_{NH_3}/J_{NH_4^+}|$ would have to be $>10^{(7.5-9.2)} = 2/100$ (see Table 1). Because $|J_{NH_3}/J_{NH_4^+}|$ cannot simultaneously be <0.5/100 and >2/100, we can conclude that an NH_4^+ efflux, regardless of mechanism, cannot account for the slow pH_i increase.

Model E: Might Endogenous Na–H Exchange Cause pH_i to Rise Following Withdrawal of High Levels of NH_3/NH_4^+?—After an intracellular acid load induced by exposure to CO_2 or butyric acid, *Xenopus* oocytes not heterologously expressing acid-base transporters have very low rates of acid extrusion (Romero et al. 1997; Grichtchenko et al. 2001; Piermarini et al. 2007). Thus, the pH_i recovery occurs only after removal of NH_3/NH_4^+. Furthermore, by analogy to the argument made in the previous section's point B (see Fig. 7b), the extrusion of H^+ would have produced a fall in pH_S, rather than the small overshoot that we observed (Fig. 2). Thus, acid extrusion by an endogenous transporter also cannot account for the pH_i recovery.

Model F: Might the Activation (or Inactivation) of Cytosolic H^+ Production Cause the Fall (or rise) in pH_i Caused by the Application (or Removal) of Extracellular NH_3/NH_4^+?—Although we can rule out NH_4^+ or H^+ uptake as an explanation for the paradoxical pH_i decrease caused by the application of 5 mM NH_3/NH_4^+ (and presumably higher concentrations as well)—and NH_4^+ or H^+ efflux as an explanation for the paradoxical pH_i increase caused by removal of high levels of NH_3/NH_4^+—we have no definitive explanation for either pH_i change. Others have proposed that members of the Rh family function as NH_3/NH_4^+ sensors in determining the choice of slug vs. culmination in *Dictyostelium discoideum* (Kirsten et al. 2005, 2008; Singleton et al. 2006). We propose that oocytes have a low-affinity "sensor" that responds, directly or indirectly, to extracellular NH_3/NH_4^+. This oocyte sensor could be either at the outer surface of the plasma membrane or somewhere reasonably close to the inner surface, but ultimately must act in two ways. (a) The sensor triggers the production of cytosolic H^+—perhaps by a metabolic pathway. The influx of NH_3 would temper the fall in pH_i and lead to the formation of some NH_4^+, which also would temper the depolarization by reducing the inwardly directed NH_4^+ diffusion potential. Indeed, AmtB reduces the depolarization (compare AmtB vs. H_2O bars in Fig. 4d and h). However, ultimately, the overwhelming majority of the incoming NH_3 must be trapped as NH_4^+ in a presumably acidic intracellular compartment. (b) The oocyte sensor triggers the slow activation of a channel permeable to NH_4^+. We have no data to address the issue of whether this activation requires the attendant fall in pH_i, or whether the putative increase in NH_4^+ permeability and the observed fall in pH_i are totally independent. Note that NH_4^+ need not enter in order to depolarize the cell. We suggest that removal of extracellular NH_3/NH_4^+ reverses this production, leading to consumption of H^+ and thus the recovery of pH_i. Because the pH_i recovery begins so soon after NH_3/NH_4^+ removal, we suggest that the NH_3/NH_4^+ sensor faces the extracellular fluid.

[4]Assuming that the NH_4^+-conductive pathway remained activate and that substantial NH_4^+ were present in the cytosol, the removal of extracellular NH_4^+ would create a diffusion potential that would drive V_m to well below the pre-NH_3/NH_4^+ value. Instead, we observed a V_m minimal undershoot that decayed rapidly, presumably reflecting either NH_4^+ efflux per se, or NH_3 efflux followed by the cytosolic reaction $NH_4^+ \rightarrow NH_3 + H^+$. We have no data that bear on the decay of the presumed NH_4^+ conductance.

V_m Changes

As noted earlier, the slowly developing depolarization that develops in the presence of NH_3/NH_4^+ could reflect permeability to NH_4^+, as suggested by others (Burckhardt and Frömter 1992). It is interesting to note that, at both 5 mM and 0.5 mM NH_3/NH_4^+, expression of AmtB substantially reduced the NH_3/NH_4^+-induced depolarization (Fig. 4d and h) without significantly affecting pH_i (Fig. 4b and f). We hypothesize that the additional influx of NH_3 through AmtB leads to the formation of modest amounts of NH_4^+ immediately beneath the plasma membrane, reducing the diffusion gradient for NH_4^+.

Possible Benefits of the Oocyte's Unusual Handling of NH_3/NH_4^+

An intriguing question that remains is why the oocyte should handle NH_3 in such an unusual manner. One possibility is that the oocyte's responses to extracellular NH_3/NH_4^+ are an adaptation that protects the cell—and perhaps, more importantly, its developmental program — from the appearance of NH_3 in pond water that contains decaying organic matter and thus NH_3/NH_4^+. Levels up to at least 0.5 mM NH_3/NH_4^+ cause no discernible changes in pH_i, and even much higher levels lead, at most, to modest, slow, and fully reversible pH_i changes. In a more typical response, an exposure to NH_3/NH_4^+ might mimic the rise in pH_i caused by the fertilization of a *Xenopus* oocyte (Webb and Nuccitelli 1981; Nuccitelli et al. 1981). The *Xenopus* oocyte seems to be particularly adept at avoiding NH_3/NH_4^+-induced pH_i increases.

Acknowledgments

This work was supported by grants from the Office of Naval Research (1N000140810532 to W·F.B.) and the National Institutes of Health (NINDS 1 P30-NS052519 to K.L.B.). At Yale University, we thank Duncan Wong for computer support. We thank Mark D. Parker for helpful discussions, Dale Huffman for engineering assistance, and Charleen Bertolini for administrative support.

References

Aickin CC, Thomas RC. An investigation of the ionic mechanism of intracellular pH regulation in mouse soleus muscle fibres. J Physiol (Lond) 1977;273:295–316. [PubMed: 23428]

Andrade SL, Dickmanns A, Ficner R, Einsle O. Crystal structure of the archaeal ammonium transporter Amt-1 from Archaeoglobus fulgidus. Proc Natl Acad Sci USA 2005;102:14994–14999. [PubMed: 16214888]

Bakouh N, Benjelloun F, Hulin P, Brouillard F, Edelman A, Chérif-Zahar B, Planelles G. NH3 is involved in the NH4+ transport induced by the functional expression of the human Rh C glycoprotein. J Biol Chem 2004;279:15975–15983. [PubMed: 14761968]

Bakouh N, Benjelloun F, Cherif-Zahar B, Planelles G. The challenge of understanding ammonium homeostasis and the role of the Rh glycoproteins. Transfus Clin Biol 2006;13:139–146. [PubMed: 16564724]

Boron WF, De Weer P. Active proton transport stimulated by CO_2/HCO_3^- blocked by cyanide. Nature 1976a;259:240–241. [PubMed: 2874]

Boron WF, De Weer P. Intracellular pH transients in squid giant axons caused by CO_2, NH_3 and metabolic inhibitors. J Gen Physiol 1976b;67:91–112. [PubMed: 1460]

Burckhardt BC, Frömter E. Pathways of NH_3/NH_4^+ permeation across Xenopus laevis oocyte cell membrane. Pflügers Arch 1992;420:83–86.

Chesler M. Regulation of intracellular pH in reticulospinal neurones of the lamprey, Petromyzon Marinus. J Physiol (Lond) 1986;381:241–261. [PubMed: 3040962]

Conroy MJ, Durand A, Lupo D, Li XD, Bullough PA, Winkler FK, Merrick M. The crystal structure of the Escherichia coli AmtB-GlnK complex reveals how GlnK regulates the ammonia channel. Proc Natl Acad Sci USA 2007;104:1213–1218. [PubMed: 17220269]

De Hemptinne A, Huguenin F. The influence of muscle respiration and glycolysis on surface and intracellular pH in fibres of the rat soleus. J Physiol 1984;347:581–592. [PubMed: 6707968]

Endeward V, Musa-Aziz R, Cooper GJ, Chen L, Pelletier MF, Virkki LV, Supuran CT, King LS, Boron WF, Gros G. Evidence that Aquaporin 1 is a major pathway for CO2 transport across the human erythrocyte membrane. FASEB J 2006;20:1974–1981. [PubMed: 17012249]

Fabiny JM, Jayakumar A, Chinault AC, Barnes EM Jr. Ammonium transport in Escherichia coli: localization and nucleotide sequence of the amtA gene. J Gen Microbiol 1991;137(Pt 4):983–989. [PubMed: 1856684]

Fagotto F. Regulation of yolk degradation, or how to make sleepy lysosomes. J Cell Sci 1995;108(Pt 12): 3645–3647. [PubMed: 8719870]

Fagotto F, Maxfield FR. Changes in yolk platelet pH during *Xenopus laevis* development correlate with yolk utilization. A quantitative confocal microscopy study. J Cell Sci 1994a;107:3325–3337. [PubMed: 7706389]

Fagotto F, Maxfield FR. Yolk platelets in *Xenopus* oocytes maintain an acidic internal pH which may be essential for sodium accumulation. J Cell Biol 1994b;125:1047–1056. [PubMed: 8195288]

Grichtchenko II, Choi I, Zhong X, Bray-Ward P, Russell JM, Boron WF. Cloning, characterization, and chromosomal mapping of a human electroneutral Na^+-driven Cl-HCO_3 exchanger. J Biol Chem 2001;276:8358–8363. [PubMed: 11133997]

Grzesiek S, Bax A. The importance of not saturating H_2O in protein NMR - application to sensitivity enhancement and NOE measurements. J Am Chem Soc 1993;115:12593–12594.

Harvey EN. Studies on the permeability of cells. J Exp Zool 1911;10:507–556.

Jacobs MH. The influence of ammonium salts on cell reaction. J Gen Physiol 1922;5:181–188. [PubMed: 19871986]

Kanamori K, Ross BD, Tropp J. Selective, in vivo observation of [5-N-15]glutamine amide protons in rat-brain by H-1-N-15 heteronuclear multiple-quantum-coherence transfer NMR. J Magnet Reson Ser B 1995;107:107–115.

Keicher E, Meech R. Endogenous Na^+ -K^+ (or NH_4^+)-2Cl^-cotransport in Rana oocytes; anomalous effect of external NH_4 + on pH_i. J Physiol 1994;475:45–57. [PubMed: 8189392]

Khademi S, Stroud RM. The Amt/MEP/Rh family: structure of AmtB and the mechanism of ammonia gas conduction. Physiology (Bethesda) 2006;21:419–429. [PubMed: 17119155]

Khademi S, O'Connell J, Remis J, Robles-Colmenares Y, Miericke LJW, Stroud RM. Mechanism of ammonia transport by Amt/MEP/Rh: Structure of AmtB at 1.35 angstrom. Science 2004;305:1587–1594. [PubMed: 15361618]

Kikeri D, Sun A, Zeidel ML, Hebert SC. Cell membranes impermeable to NH_3. Nature 1989;339:478–480. [PubMed: 2725680]

Kirsten JH, Xiong Y, Dunbar AJ, Rai M, Singleton CK. Ammonium transporter C of *Dictyostelium discoideum* is required for correct prestalk gene expression and for regulating the choice between slug migration and culmination. Dev Biol 2005;287:146–156. [PubMed: 16188250]

Kirsten JH, Xiong Y, Davis CT, Singleton CK. Subcellular localization of ammonium transporters in *Dictyostelium discoideum*. BMC Cell Biol 2008;9:71. [PubMed: 19108721]

Lu J, Daly CM, Parker MD, Gill HS, Piermarini PM, Pelletier MF, Boron WF. Effect of human carbonic anhydrase II on the activity of the human electrogenic Na/HCO_3 cotransporter NBCe1-A in Xenopus oocytes. J Biol Chem 2006;281:19241–19250. [PubMed: 16687407]

Musa-Aziz R, Chen L, Pelletier MF, Boron WF. Relative CO_2/NH_3 selectivities of AQP1, AQP4, AQP5, AmtB and RhAG. Proc Natl Acad Sci USA. 2009 in press.

Nuccitelli R, Webb DJ, Lagier ST, Matson GB. ^{31}P NMR reveals increased intracellular pH after fertilization in Xenopus eggs. Proc Natl Acad Sci USA 1981;78:4421–4425. [PubMed: 6945594]

Overton E. Über die osmotischen Eigenschaften der Zelle in ihrer Bedeutung fur die Toxicologie und Pharmacologie. Z Phys Chem 1897;22:189–209.

Parker MD, Musa-Aziz R, Rojas JD, Choi I, Daly CM, Boron WF. Characterization of human SLC4A10 as an electroneutral Na/HCO3 cotransporter (NBCn2) with Cl–self-exchange activity. J Biol Chem 2008;283:12777–12788. [PubMed: 18319254]

Patel AB, de Graaf RA, Mason GF, Rothman DL, Shulman RG, Behar KL. The contribution of GABA to glutamate/glutamine cycling and energy metabolism in the rat cortex in vivo. Proc Natl Acad Sci USA 2005;102:5588–5593. [PubMed: 15809416]

Piermarini PM, Choi I, Boron WF. Cloning and characterization of an electrogenic Na/HCO_3 cotransporter from the squid giant fiber lobe. Am J Physiol Cell Physiol 2007;292:C2032–C2045. [PubMed: 17267543]

Piotto M, Saudek V, Sklenar V. Gradient-tailored excitation for single-quantum NMR-spectroscopy of aqueous solutions. J Biomol NMR 1992;2:661–665. [PubMed: 1490109]

Romero MF, Hediger MA, Boulpaep EL, Boron WF. Expression cloning and characterization of a renal electrogenic Na^+/HCO_3^- cotransporter. Nature 1997;387:409–413. [PubMed: 9163427]

Romero MF, Fong P, Berger UV, Hediger MA, Boron WF. Cloning and functional expression of rNBC, an electrogenic Na^+/HCO_3^- cotransporter from rat kidney. Am J Physiol 1998;274:F425–F432. [PubMed: 9486238]

Roos A, Boron WF. Intracellular pH. Physiol Rev 1981;61:296–434. [PubMed: 7012859]

Shaka AJ, Keeler J, Frenkiel T, Freeman R. An improved sequence for broad-band decoupling—waltz–16. J Magnet Reson 1983;52:335–338.

Singh SK, Binder HJ, Geibel JP, Boron WF. An apical permeability barrier to NH_3/NH_4^+ in isolated, perfused colonic crypts. Proc Natl Acad Sci USA 1995;92:11573–11577. [PubMed: 8524806]

Singleton CK, Kirsten JH, Dinsmore CJ. Function of ammonium transporter A in the initiation of culmination of development in *Dictyostelium discoideum*. Eukaryot Cell 2006;5:991–996. [PubMed: 16835443]

Soupene E, Lee H, Kustu S. Ammonium/methylammonium transport (Amt) proteins facilitate diffusion of NH_3 bidirectionally. Proc Natl Acad Sci USA 2002;99:3926–3931. [PubMed: 11891327]

Toye AM, Parker MD, Daly CM, Lu J, Virkki LV, Pelletier MF, Boron WF. The human NBCe1-A mutant R881C, associated with proximal renal tubular acidosis, retains function but is mistargeted in polarized renal epithelia. Am J Physiol Cell Physiol 2006;291:C788–C801. [PubMed: 16707554]

Waisbren SJ, Geibel JP, Modlin IM, Boron WF. Unusual permeability properties of gastric gland cells. Nature 1994;368:332–335. [PubMed: 8127367]

Warburg EJ. Studies on carbonic acid compounds and hydrogen ion activities in blood and salt solutions. A contribution to the theory of the equation of Lawrence J. Henderson and K.A. Hasselbalch. Biochem Z 1922;16:153–340.

Webb DJ, Nuccitelli R. Direct measurement of intracellular pH changes in Xenopus eggs at fertilization and cleavage. J Cell Biol 1981;91:562–567. [PubMed: 6796594]

Zheng L, Kostrewa D, Berneche S, Winkler FK, Li XD. The mechanism of ammonia transport based on the crystal structure of AmtB of Escherichia coli. Proc Natl Acad Sci USA 2004;101:17090–17095. [PubMed: 15563598]

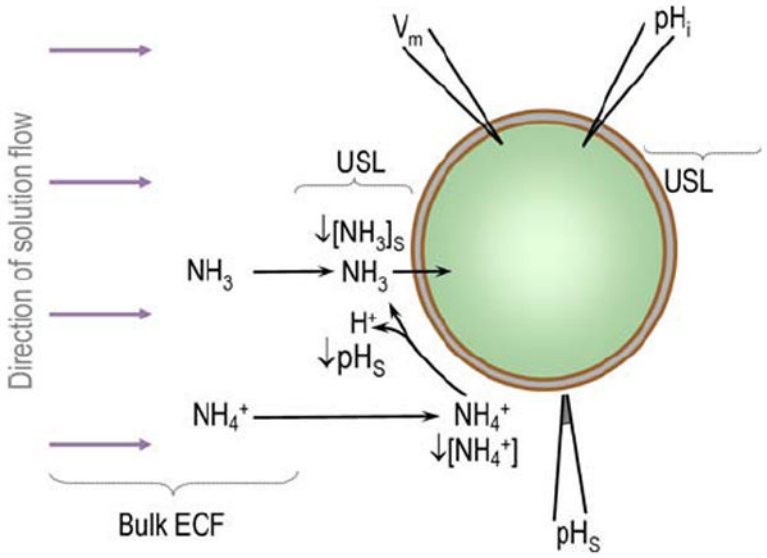

Fig. 1.

Model of an oocyte exposed to NH_3/NH_4^+. The large purple arrows indicate the directon of bulk solution flow. *USL* unstirred layer; *Bulk ECF* bulk extracellular fluid

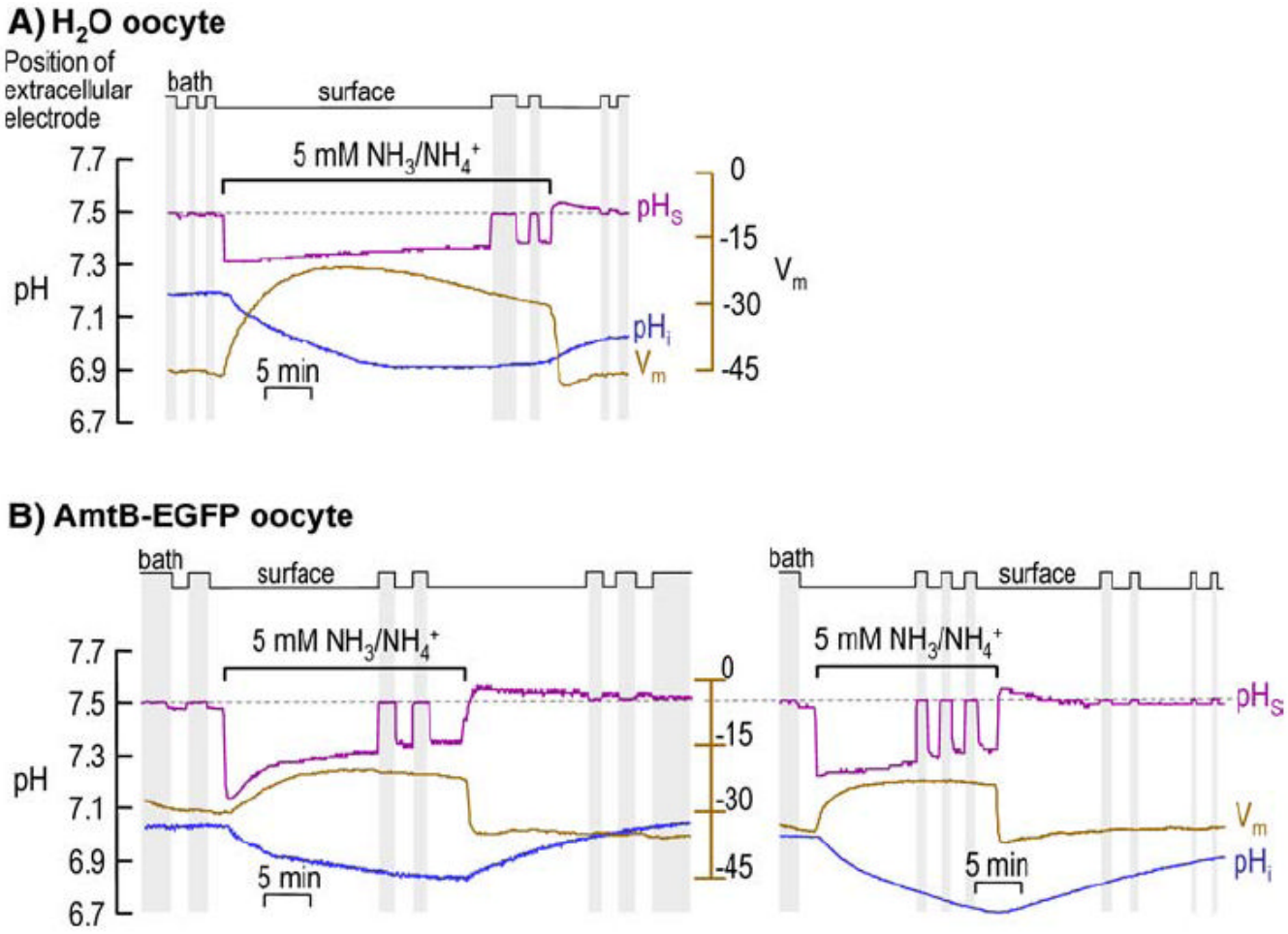

Fig. 2.

Intracellular pH (pH_i) and surface (pH_S) records during application and removal of 5 mM NH_3/NH_4^+. **a** H_2O-injected oocyte. **b** AmtB EGFP-tagged expressing oocytes. At the indicated times, we switched the extracellular solution from ND96 to 5 mM NH_3/NH_4^+ and then back again. **b** shows two representative experiments: on the left, pH_S at first decays rapidly and then more slowly, whereas on the right, pH_S decays slowly throughout the NH_3/NH_4^+ exposure. In both **a** and **b**, the purple record is pH_S, the blue record is pH_i, and the brown record is V_m. The vertical gray bands represent periods during which the pH_S electrode was moved to the bulk ECF for calibration (fixed pH of 7.50). In H_2O oocytes, mean pH_i was 7.10 ± 0.04 before and 6.84 ± 0.06 during exposure to 5 mM NH_3/NH_4^+ (n = 6; p = 0.005); the comparable mean V_m values were −43 ± 2 and − 25 ± 2 mV (n = 6; p = 0.0002). In AmtB oocytes, the mean pH_i was 7.14 ± 0.04 before and 6.98 ± 0.06 during exposure to 5 mM NH_3/NH_4^+ (n = 8; p = 0.037); the comparable mean V_m values were −38 ± 4 and −26 ± 2 (n = 8; p = 0.010)

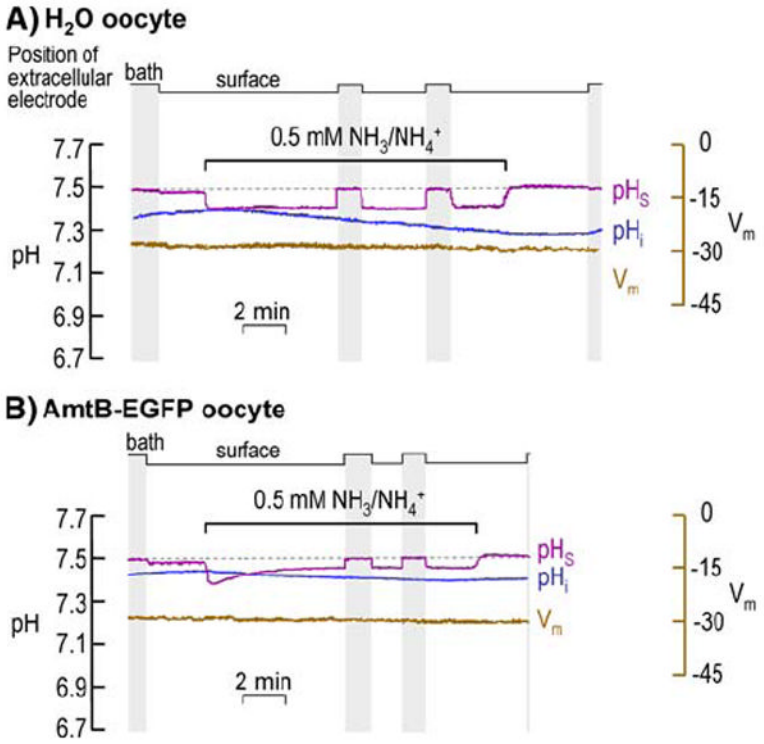

Fig. 3.

Intracellular pH (pH_i) and surface (pH_S) records during application and removal of 0.5 mM NH_3/NH_4^+. **a** AmtB EGFP-tagged expressing oocyte. **b** H_2O-injected oocyte. At the indicated times, we switched the extracellular solution from ND96 to 0.5 mM NH_3/NH_4^+ and then back again. In both **a** and **b**, the purple record is pH_S, the blue record is pH_i, and the brown record is V_m. The vertical gray bands represent periods during which the pH_S electrode was moved to the bulk ECF for calibration (fixed pH of 7.50). In H_2O oocytes, the mean pH_i was 7.21 ± 0.05 before and 7.17 ± 0.05 during exposure to 0.5 mM NH_3/NH_4^+ (n = 8; p = 0.61); the comparable mean V_m values were −44 ± 2 and -40 ± 2 mV (n = 8; p = 0.14). In AmtB oocytes, the mean pH_i was 7.24 ± 0.05 before and 7.21 ± 0.05 during exposure to 0.5 mM NH_3/NH_4^+ (n = 8; p = 0.52); the comparable mean V_m values were −31 ± 4 and −30 ± 4 (n = 8; p = 0.87)

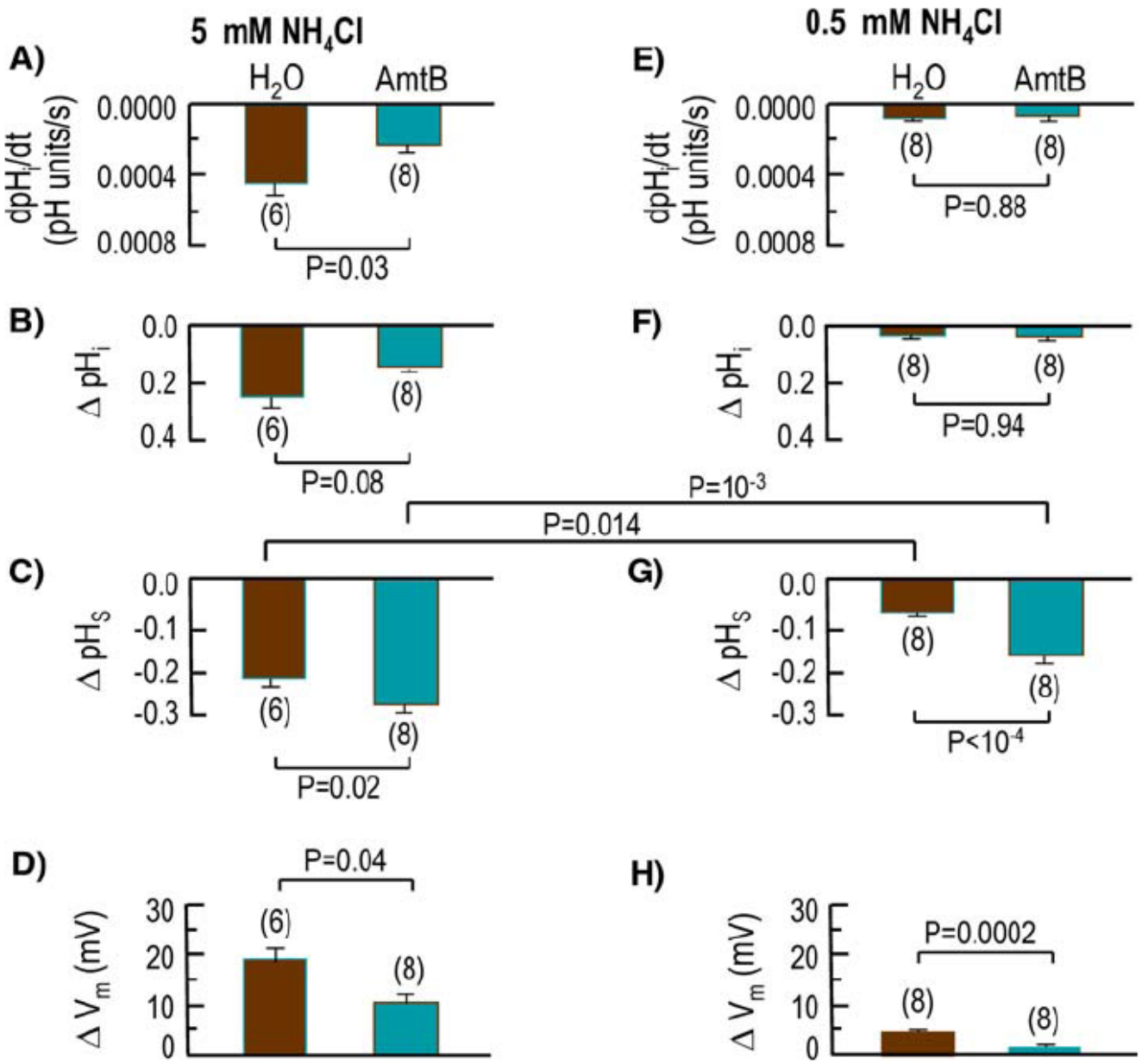

Fig. 4.

Summary of the mean initial rate of pH_i decrease (dpH_i/dt) and magnitude of the NH_3-induced change in steady-state pH_i (ΔpH_i), ΔpH_S, and V_m for larger groups of experiments like those in Figs. 2 and 3

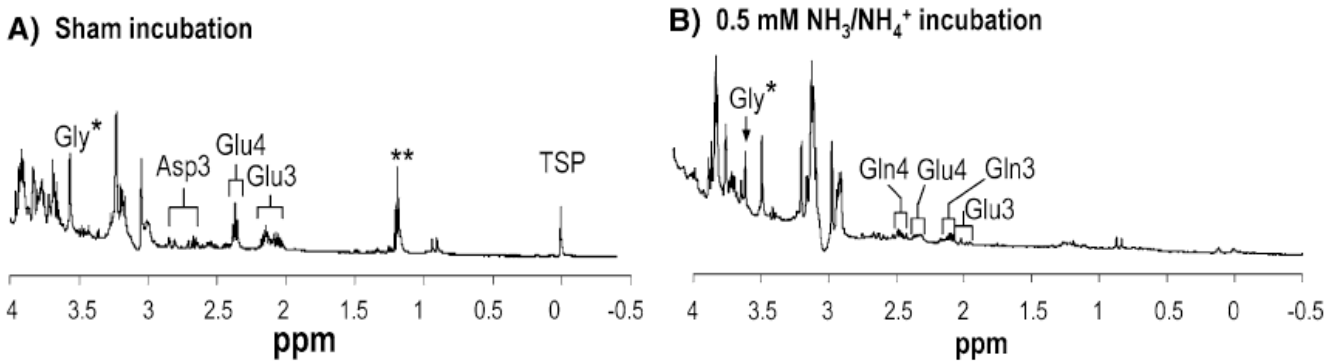

Fig. 5.

^{1}H-NMR spectra of ethanol extracts of oocytes. **a** Sham incubation (i.e., oocytes not exposed to NH_3/NH_4^+). **b** Oocytes incubated with 0.5 mM $^{15}NH_3/^{15}NH_4^+$ for 10 min. Each spectrum represents the extract of 20 oocytes. TSP, 3-trimethylsilyl-[2,2,3,3-d_4]-propionate(Na^+), was added as a chemical-shift reference (0.0 ppm). *Glycine was added during oocyte extraction to serve as an internal concentration standard and to control for potential metabolite losses. **Residual ethanol contaminant remaining after extraction. Estimated concentrations of metabolites in control noninjected oocytes not exposed to NH_3/NH_4^+. (A) Glutamate (Glu): 6.48 mM. Estimated metabolite concentrations after incubation with $^{15}NH_3/^{15}NH_4^+$ for 10 min: Glu: H_2O, 1.69 mM. Glutamine (Gln): 1.1 mM. Glu and Gln methylene protons (H_4 and H_3) and lactate methyl protons (H_3) are depicted. Glu H_4 and H_3 were observed in control noninjected oocytes incubated with $^{15}NH_3/^{15}NH_4^+$

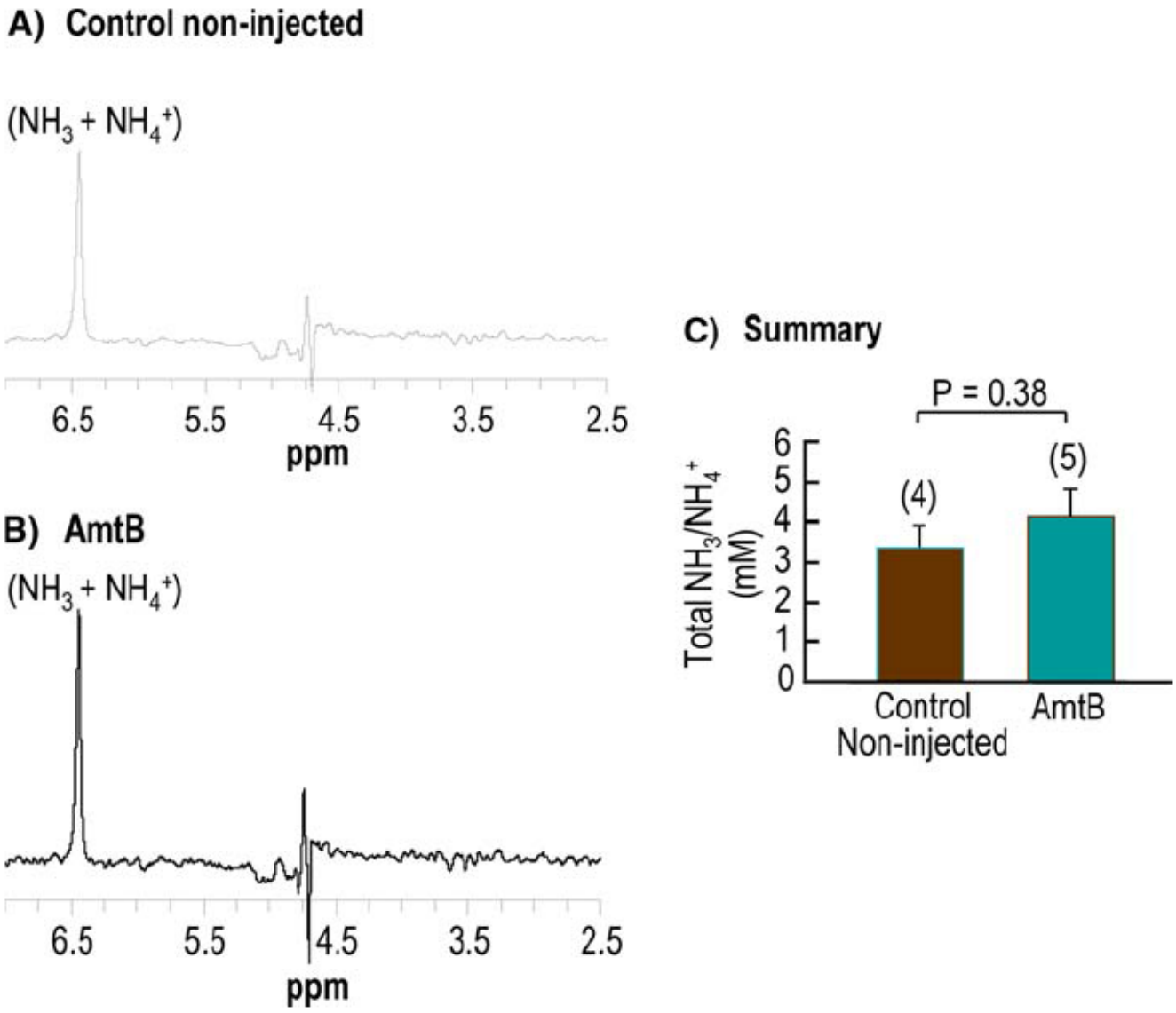

Fig. 6.

Representative ^{1}H-^{15}N HSQC spectra of *Xenopus* oocytes incubated with $^{15}NH_3/^{15}NH_4^+$. **a** Control noninjected oocytes. **b** AmtB oocytes. Total ammonia appears as a single resonance at ~6.5 ppm (relative to water, assigned to 4.7 ppm). Spectral intensities were scaled relative to the intensity of 0.5 mM ^{15}N-ammonia in the incubation medium of each sample acquired with the same pulse parameter settings. The residual water signal artifact appears at 4.7 ppm. **c** Total ammonia ($NH_3 + NH_4^+$) concentration in control noninjected and in AmtB oocytes. Values are mean ± SE, with numbers of oocyte samples for each group in parentheses. The statistical comparisons were made using unpaired two-tailed *t*-tests. The experimental error was large due to fast evaporation of the ammonia in both the standard solution and the extracts

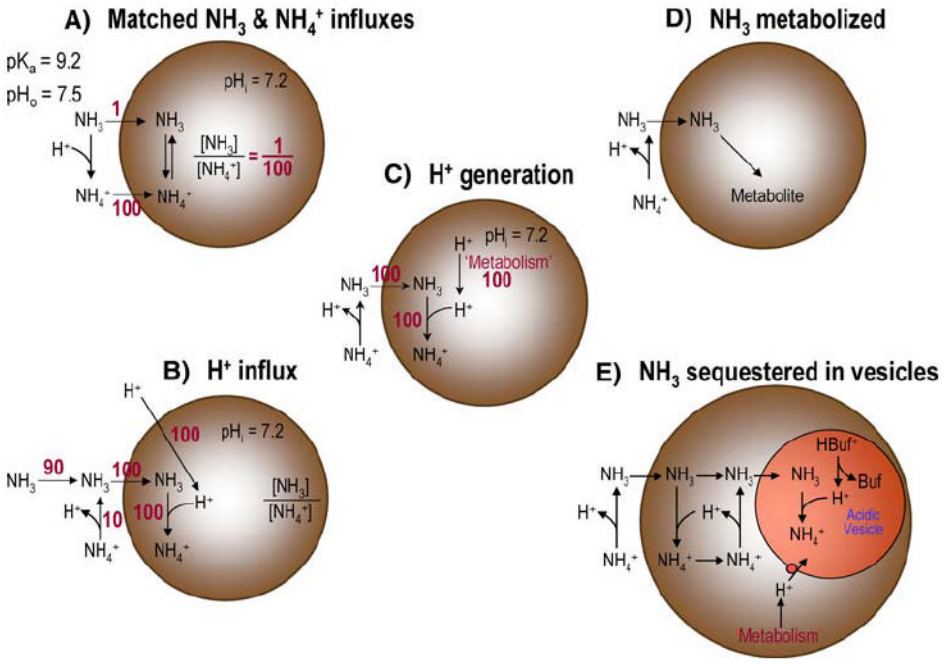

Fig. 7.
Models of NH_3/NH_4^+ handling by *Xenopus* oocytes

Table 1

Predicted pH changes

Condition	Effect on compartment from which NH_3 and NH_3/NH_4^+ leave	Effect on compartment that NH_3 and NH_3/NH_4^+ enter
$pH < pH_{Null}$ … that is, $J_{NH_3}/J_{NH_4^+} > (J_{NH_3}/J_{NH_4^+})_{Null}$	↓pH	↑pH
$pH = pH_{Null}$ … that is, $J_{NH_3}/J_{NH_4^+} = (J_{NH_3}/J_{NH_4^+})_{Null}$	⧚pH	⧚pH
$pH > pH_{Null}$ … that is, $J_{NH_3}/J_{NH_4^+} < (J_{NH_3}/J_{NH_4^+})_{Null}$	↑pH	↓pH

Note. ↓pH, decrease in pH; ↑pH, increase in pH; ⧚pH, no pH change in this compartment